Journal of Power Sources 266 (2014) 1–6

Contents lists available at ScienceDirect

Journal of Power Sources

journal homepage: www.elsevier.com/locate/jpowsour

Mica-like vanadium pentoxide-nanostructured thin film as high-performance cathode for lithium-ion batteries

Danmei Yu [a,*], Yajuan Qiao [a], Xiaoyuan Zhou [b], Jie Wang [a], Chao Li [a], Changguo Chen [a], Qisheng Huo [c]

[a] School of Chemistry and Chemical Engineering, Chongqing University, Chongqing 400044, PR China
[b] School of Physics, Chongqing University, Chongqing 400044, PR China
[c] State Key Laboratory of Inorganic Synthesis and Preparative Chemistry, College of Chemistry, Jilin University, Changchun 130012, PR China

HIGHLIGHTS

- Mica-like V_2O_5 nanostructured thin-film is fabricated directly by anodic electrodeposition.
- Mica-like V_2O_5 thin-films are formed by nanosheets with thickness less than 50 nm.
- The initial discharge capacity of V_2O_5 thin-film was 596 mAh g^{-1} at 1080 mA g^{-1}.
- The fading rate of V_2O_5 thin-film was 1% per cycle at 1080 mA g^{-1}.

GRAPHICAL ABSTRACT

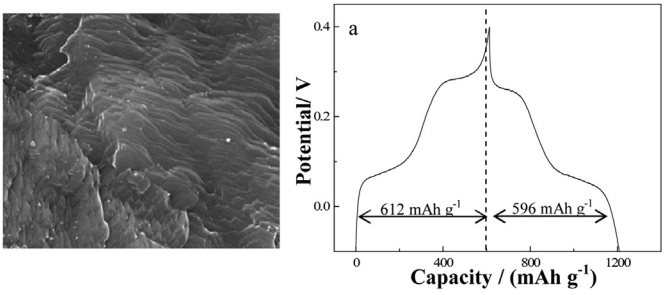

ARTICLE INFO

Article history:
Received 2 March 2014
Received in revised form
17 April 2014
Accepted 17 April 2014
Available online 10 May 2014

Keywords:
Mica-like
Nanostructure
Vanadium pentoxide
Thin film
Lithium-ion batteries
Cathode materials

ABSTRACT

Stable and homogeneous mica-like vanadium pentoxide (V_2O_5)-nanostructured thin films are prepared directly by simple anodic deposition from V_2O_5/H_2O_2 sol solution, and then dried at ambient temperature and annealed at 500 °C in air for 1 h. The films' crystal- and microstructures, surface morphology and Li-ion intercalation properties were characterized and analyzed by X-Ray diffraction (XRD), field emission scanning electron microscopy (FSEM), thermogravimetric analysis (TGA), and electrochemical techniques. When used as a lithium-ion battery (LIB) cathode, the films exhibit a large discharge capacity of 596 mAh g^{-1} at a current density of 1080 mA g^{-1}, as well as excellent cyclic stability and a fading rate of 1% per cycle. Explanations for such significant enhancements in specific capacity, cyclic stability, and rate performance of mica-like V_2O_5-nanostructured thin films are demonstrated in this study.

1. Introduction

In recent years, both environmental and energy-resource-depletion issues have made energy conversion and storage top concerns. More environmentally benign and sustainable energy-storage systems, accordingly, are the desired future power sources [1]. In this regard, lithium-ion batteries (LIBs), with their high power output, long cycle life and high energy density, represent an attractive option for many researchers. LIBs have already been used in a wide range of applications including portable electronic devices, electric vehicles, and implantable medical devices [2–4]. The key to LIB performance enhancement, obviously, is the development of new and improved cathode materials. The maximum

* Corresponding author. Tel.: +86 023 65111357.
E-mail address: yudanmei@cqu.edu.cn (D. Yu).

http://dx.doi.org/10.1016/j.jpowsour.2014.04.099
0378-7753/

practical discharge capacity of the commercially available cathode materials available for LIBs, such as $LiCoO_2$ [5–6], $LiNiO_2$ [7], $LiMn_2O_4$ [8], $LiFePO_4$ [9,10], and their derivatives [11–13], at present, is ~300 mAh g^{-1}. However, $LiCoO_2$ toxicity and high cost have introduced environmental problems and made LIBs more expensive, while the utility of commercial $LiNiO_2$ is severely curtailed owing to its low specific capacity and insufficient cycle life. And as for $LiMn_2O_4$ cathode materials, they have been found to suffer from a severe capacity-fading problem [14].

More recently, vanadium pentoxide (V_2O_5) of a layered structure has been considered a promising LIB cathode electrode material owing to its high discharge capacity, low cost and abundance [15]. However, its poor structural stability, low electronic conductivity and slow electrochemical kinetics have hampered its LIB application. In efforts to accelerate the electrochemical kinetics, much research has focused on the synthesis and fabrication of nanostructured vanadium oxides [16]. And in fact, single-crystal V_2O_5 nanorod arrays, nanotubes, nanoroll and nanocables have been demonstrated to possess significantly enhanced electrochemical Li-ion intercalation properties [17]. Such improvement has been attributed to nanostructured materials providing shorter and simpler diffusion paths for lithium ions and allowing maximal freedom for the dimension change that accompanies lithium-ion intercalation and de-intercalation.

Among the many nanomaterial fabrication methods, which include hydrothermal treatment, the template-based method, the electrospinning method, and others, the electrodeposition method is perhaps the most low-cost, simple and easy for industrial applications. Liu [18] reported that nanostructured V_2O_5 prepared by cathodic deposition showed, as cathodes for lithium-ion intercalation, excellent electrochemical properties: specifically, a high initial discharge capacity of 402 mAh g^{-1} with a discharging current density of 200 mA g^{-1} (1.3 C). In the present study, a modified method combining sol–gel processing with anodic electrodeposition was used to fabricate mica-like V_2O_5 nanostructured thin-film electrodes. Such film in LIB applications offers the large discharge capacity of 596 mAh g^{-1} (at a current density of 1080 mA g^{-1}), which is much higher than that of V_2O_5 film prepared by the cathodic deposition method, as well as excellent cyclic stability due to its unique structure and morphology. The characteristics of the crystal structure and morphology of the V_2O_5 thin films, and their electrochemical performances, additionally, were systematically studied.

2. Experimental

According to the procedure reported by Fontenot et al. [19], V_2O_5 powder (Shanghai Shenjiang Chemical Factory) was added to a solution of 30% H_2O_2 ($n(V_2O_5):n(H_2O_2) = 1:12.25$) and de-ionized water at room temperature and stirred vigorously until the complete dissolution of V_2O_5 yielded, after 60 min, a clear dark red liquid. This sol was further dispersed and then diluted to the vanadium concentration of 3.2 mol L^{-1}. In the preparation of V_2O_5 thin films, one Platinum (Pt) plate was used as the deposition substrate on the positive side, and another as a counter electrode on the negative side. The distance between the electrodes was maintained constant at 2.5 cm while 10 min of electrodeposition was carried out; the deposition area of the positive electrode was 0.5 cm^2, and the deposition voltage was 5 V. The thin films were dried in air completely over 12 h in order to prevent cracking from the drastic volume change; subsequently they were annealed in a 500 °C ambient atmosphere for 1 h followed by a slow cool-down. All of the samples finally were stored in air preparatory to characterizations and performance measurements.

The crystal phases and crystallite sizes of the V_2O_5 thin films were characterized by X-ray diffraction (XRD, Japan Shimadzu, XRD-6000), and their surface morphologies were examined under field emission scanning electron microscopy (FESEM, JSM-7100F). The films' thermogravimetric properties, meanwhile, were investigated by thermogravimetric analysis (TGA; Shimadzu DTG-60H thermal analyser) in air, from room temperature to 600 °C at the heating rate of 10 °C per minute.

The electrochemical performances of the V_2O_5 thin-film electrodes were tested at room temperature using a standard three-electrode system: 1 mol L^{-1} $LiClO_4$ in propylene carbonate (PC) as the electrolyte, a Pt plate as the counter electrode, and Ag/AgCl as the reference electrode. Cyclic voltammetric (CV) tests on the electrodes were carried out between −0.2 V and 0.6 V (*vs.* Ag/AgCl) at a scan rate of 5 mV s^{-1}, and their charge–discharge properties were investigated by chronopotentiometric (CP) measurement within the −0.1 V to 0.4 V range (*vs.* Ag/AgCl) for various current densities. Both the CV tests and CP measurements were performed using an electrochemical analyzer (CH Instruments, Model 660B).

3. Results and discussion

Fig. 1 compares the XRD patterns of as-deposited V_2O_5 films prepared by anodic deposition from sol solution at room temperature and with those annealed at 500 °C in air for 1 h. As is apparent, the as-deposited films showed an intense (001) peak centered around 8.1° and indexed to hydrous vanadium pentoxide ($V_2O_5 \cdot nH_2O$) of layered structure, as is consistent with the literature [20,21], the broad (001) peak suggesting, moreover, an amorphous structure. The crystallite size as estimated by Scherrer Equation was 4.2 nm, and the interlayer distance calculated by Bragg's law was 10.94 Å, which indicated a crystalline water composition in this sample of $n < 1.5$ [22]. The series of (00*l*) peaks reflected the preferred orientation of a V_2O_5 layered structure effected by anodic deposition, while the missing (002) peak suggested the formation of double V_2O_5 sheets in each layer [23].

After each V_2O_5 thin-film sample was annealed at 500 °C in air for 1 h, it was completely dehydrated, thus transitioning to the pure orthorhombic phase with good crystallinity, as shown in the XRD pattern. The interlayer distance along the c-axis was calculated as 4.23 Å, slightly short relative to the crystalline structure of

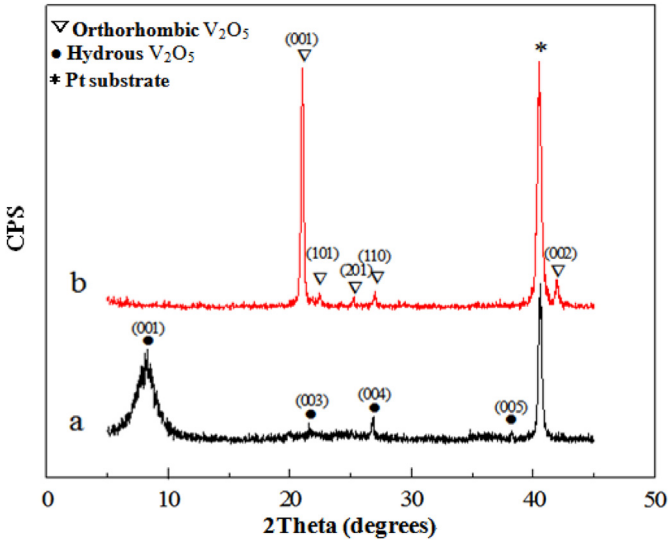

Fig. 1. XRD patterns of V_2O_5 films: a) before annealing; b) after annealing at 500 °C in air for 1 h.

orthorhombic V_2O_5 (Joint Committee on Powder Diffraction Standards [JCPDS] No. 41-1426), due to the shift of the (001) peak in the higher-angle direction. The V_2O_5 thin film is relatively well ordered for sheet materials owing to the absence of (*h*00) and (0*k*0) peaks, making reversible intercalation and de-intercalation of lithium ions much easier. Meanwhile, it was indicated that the annealed V_2O_5 thin film also has a preferred orientation, as evidenced by the missing diffraction pattern for the (0*k*0) plane along the *b*-axis. In fact, it was reported [24] that the oxygen density varies with the different crystal faces of V_2O_5, of which the oxygen density of the (*h*00) crystal face is the largest. Thus, the absent (*h*00) peaks demonstrated that there are oxygen defects in the crystal structure of V_2O_5 thin film. The crystallite size of the anodic-electrodeposited 500 °C-annealed orthorhombic V_2O_5 thin film was calculated to 32.1 nm, according to the XRD pattern in Fig. 1b.

Fig. 2 provides FESEM images of V_2O_5 thin films as-deposited and annealed at 500 °C in air for 1 h. From Fig. 2a, the V_2O_5 thin films were indeed uniform before annealing. As Fig. 2b and c shows, the V_2O_5 thin film annealed was composed of small, 1.0–2.0 μm diameter building blocks and was stably, homogeneously deposited and uniformly spread over the substrate. With respect to Fig. 2d and e, it is interesting to observe that the building blocks were

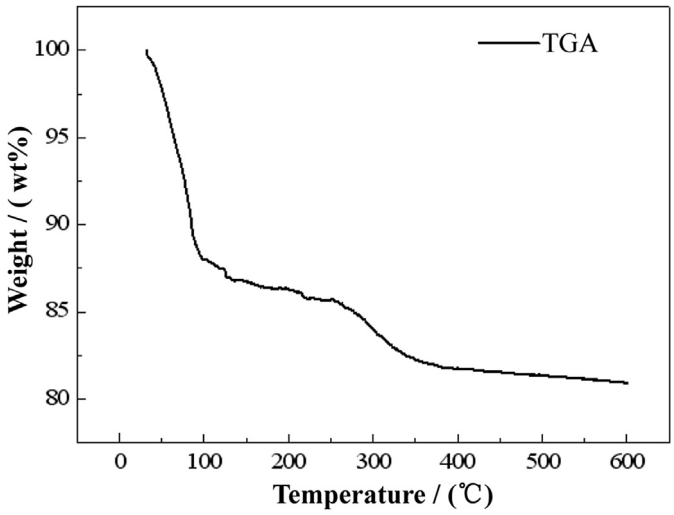

Fig. 3. TGA curve for anodic-electrodeposited V_2O_5 thin films.

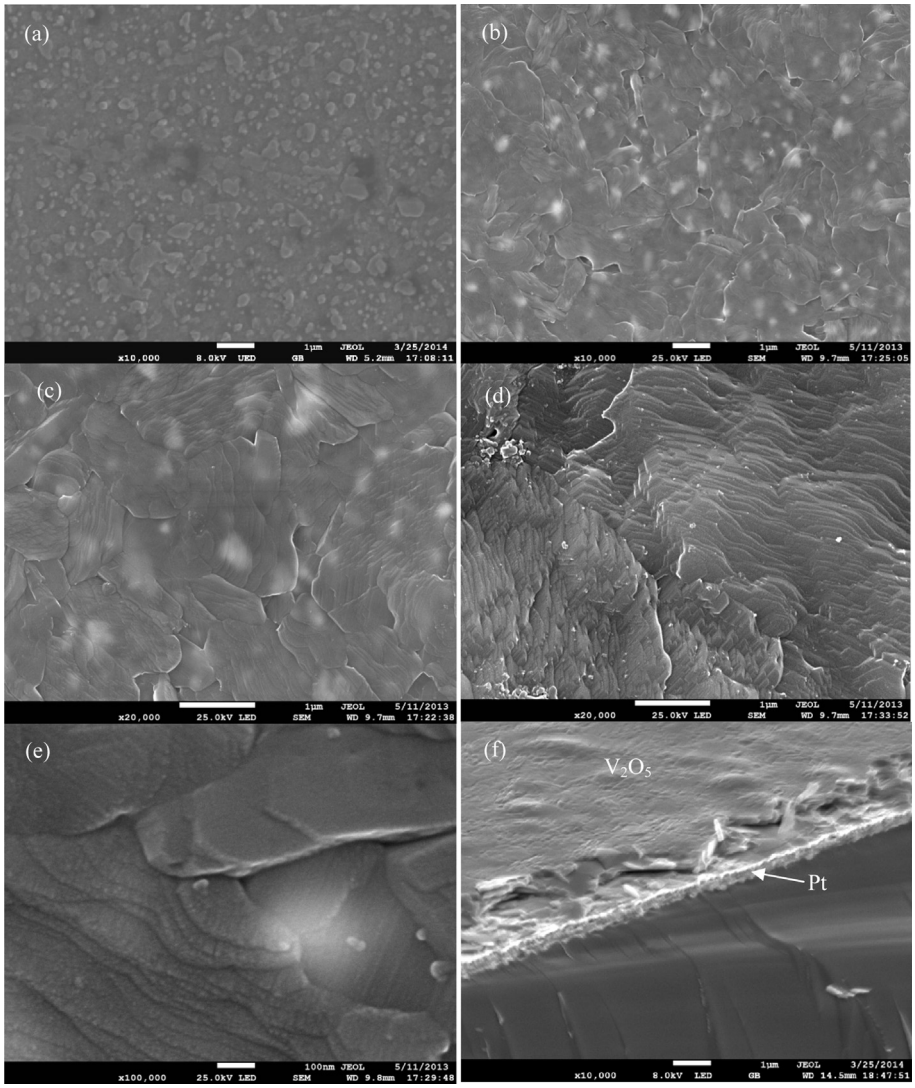

Fig. 2. FESEM images of V_2O_5 thin film (a) prior to annealing; (b), (c), (d), (e) and (f) after annealing at 500 °C in air for1 h.

formed by dozens of closely stacked V_2O_5 nanosheets of less than 50 nm thickness, as in the structure of mica. To the best of our knowledge, no mica-like V_2O_5-nanostructured thin film has been reported. It should be noted, furthermore, that due to the formation of such nanosheets in the structure of V_2O_5 thin films, the interface of the active materials on an electrode can be increased with electrolyte solution, which increase offers a high and readily accessible surface area and a shorter distance for lithium-ion intercalation/de-intercalation, thus resulting in deeper lithium-ion intercalation and a markedly increased capacity [24,25]. In addition, the film thickness was about 1 μm according to the cross section image of V_2O_5 film thin (Fig. 2f).

Fig. 3 plots the TGA curve for the anodic-electrodeposited V_2O_5 thin films. Note that the temperature range differs from those applied in earlier studies due to the differences in the respective film-processing methods utilized [18,26]. The ~13% weight loss below 100 °C can be ascribed mainly to the evaporation of free water in the V_2O_5 thin film, that between 100 °C and 250 °C, ~3%, to the loss of weakly bound water, and that between 250 °C and 400 °C, ~5%, generally to the loss of crystalline water from $V_2O_5 \cdot nH_2O$. Above 400 °C, there was no weight loss, because there was no crystalline water remaining in the film. The occurrence of V_2O_5 crystallization indicated that the V_2O_5 thin films annealed at 500 °C were crystal materials, which fact is consistent with the XRD and SEM results discussed above.

Next, the LIB-cathode electrochemical performances of the mica-like V_2O_5 thin-film electrodes were systematically investigated. Fig. 4a plots are the typical cyclic voltammogram (CV) curves based on the 5 mV s^{-1} scan rate within the −0.2 V to 0.6 V potential range (*vs.* Ag/AgCl). Each curve has two pairs of well-defined redox peaks, suggestive of the reversibility of the mica-like V_2O_5-nanostructured thin film, show noticeable improvement, and the irreversible phase transition is eliminated. Moreover, closer two pairs of peaks reflect the electrodes' enhanced lithium-ion diffusion kinetics due to the huge surface area and excessive surface energy of nanostructured materials, which characteristics offer additional sites for lithium-ion intercalation/de-intercalation and allow phase transitions that are otherwise difficult to achieve in bulk materials. The two anodic oxidation peaks were located at 0.11 V and 0.31 V in the first cycle, which correspond to the Li^+ ions' de-intercalation; the cathodic peaks were located at −0.02 V and 0.20 V, which are attributable to Li^+ intercalation accompanied by V^{5+}, which reduced to V^{4+} and then to V^{3+}. It is reported that mesoporous V_2O_5 nanofibers [26] under the same conditions, showed cathodic peaks at −0.44 V, −0.23 V and $V_2O_5 \cdot nH_2O$ xerogel films [27] at −0.3 V, −0.4 V. These results indicated that with the mica-like V_2O_5 thin-film cathode, the energy density of LIBs can be increased thanks to the improved operation potential. Fig. 4b plots CV curves for the mica-like V_2O_5-nanostructured thin film after 20 charge−discharge cycles. Compared with the first cycle, the current and potential of the redox peaks did not change dramatically, as reflected the films' excellent cyclic stability and reversibility.

Fig. 5a plots chronopotentiometric curves for the mica-like V_2O_5-nanostructured thin-film electrode under a current density of 1080 mA g^{-1} and a potential ranging from −0.1 to 0.4 V *vs.* Ag/AgCl. Evident are two well-defined plateaus in the cathodic and anodic processes from 0.05 V to 0.10 V and 0.25 V to 0.3 V, respectively. A discharge capacity of 596 mAh g^{-1} was delivered in the first cycle under a current density of 1080 mA g^{-1}, much higher than the initial discharge values for mesoporous V_2O_5 nanofibers (377 mAh g^{-1} at the current density of 625 mA g^{-1}) [26] and $V_2O_5 \cdot nH_2O$ film (275 mAh g^{-1} at the current density of 850 mA g^{-1}) reported in literature; [20] the corresponding charge capacity, meanwhile, was found to be 612 mAh g^{-1}, with an irreversible capacity of 16 mAh g^{-1}. Fig. 5b also showed that during the charge/discharge, the coulombic efficiency was almost 100% and did not change obviously with the increase of number cycle. These results are further proof of the mica-like V_2O_5-nanostructured thin films' excellent reversibility. Although $V_2O_5 \cdot nH_2O$ nanotube arrays, nanocable arrays and nanorod arrays reported on in the literature have demonstrated higher initial capacities, these performances deteriorated rapidly during the charge−discharge process [27,16]. The charge/discharge capacity of the mica-like V_2O_5-nanostructured thin films examined in the present study, by contrast, diminished only slowly (Fig. 5b) in the tenth cycle, showing a discharge capacity of 528 mAh g^{-1} and a loss rate of 1% per cycle, slightly higher than that of mesoporous V_2O_5 nanofibers with a current density of 625 mA g^{-1} [26]. As is the case for all nanostructured materials, the improvement of the intercalation/de-intercalation behavior of V_2O_5 can be attributed to high surface area and short transport distance. Nevertheless, given thin films' closely stacked mica-like V_2O_5 nanosheet structure, it is advantageous to increase lithium ions' intercalation capacity and enhance electrode-material stability during cycles. In this way, the discharge/charge capacity of V_2O_5-nanostructured thin film is greatly increased, and the attenuation of discharge capacity, significantly inhibited. It should be noted that V_2O_5 thin film examined in the present study after 500 °C annealing for 1 h was green−yellow, not the color typically observed for V_2O_5 powder or nanofiber, which is yellow [26], (V_2O_5 is yellow; VO_2 is blue) [28].

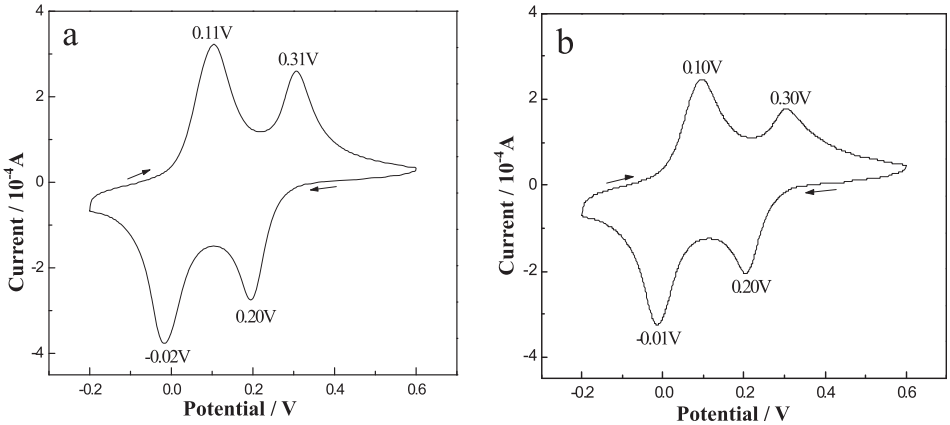

Fig. 4. CV curves for mica-like V_2O_5-nanostructured thin films prepared by anodic deposition method in (a) the first and (b) twentieth cycles, in a potential range between −0.2 V and 0.6 V *vs.* the Ag/AgCl reference electrode.

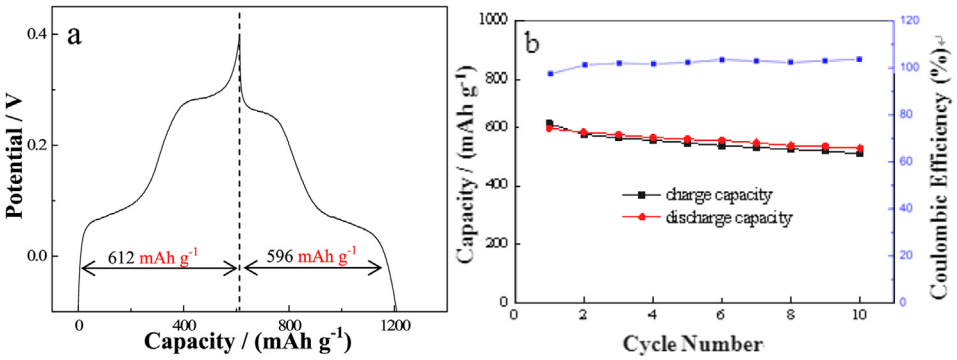

Fig. 5. (a) Chronopotentiometric curves for mica-like V_2O_5-nanostructured thin-film electrode under current density of 1080 mA g^{-1} (7.2 C) in first charge/discharge cycle, for −0.1–0.4 V potential *vs.* Ag/AgCl; (b) Discharge/charge capacity of mica-like V_2O_5-nanostructured thin-film electrode as function of cyclic number, for 1080 mA g^{-1} current density, and the coulombic efficiency curve.

The green–yellow color can be ascribed to a mixture of yellow V^{5+} and blue V^{4+}, a fact confirmed by Liu et al. [18]. The coexistence of V^{4+} and V^{5+} in V_2O_5 thin film can, as confirmed by the present XRD results, lead to the presence of oxygen vacancies. And the presence of oxygen vacancies results, in turn, in the formation of a more open structure and, thus, easier access for lithium-ion intercalation and diffusion. Oxygen vacancies, additionally, might serve as possible nucleation centers for phase transformation during the lithium-ion intercalation and de-intercalation processes [29]. The presence of lower-valence vanadium ions and the associated oxygen vacancies, moreover, might enhance the conductivity of electrode materials [30].

Fig. 6a summarizes the discharge capacity of the mica-like V_2O_5-nanostructured thin film as a function of current density. It is apparent that at fairly high current densities, which correspond to fast discharge/charge battery cycles, the thin-film electrode nonetheless retains a high discharge capacity: 623.8 mAh g^{-1} at 1080 mA g^{-1}, 386.6 mAh g^{-1} at 2210 mA g^{-1}, and 262.8 mAh g^{-1} at 4420 mA g^{-1}. As observed of all electroactive materials with respect to lithium-ion intercalation and de-intercalation, the discharge capacity of mica-like V_2O_5-nanostructured thin film decreases with increasing current density. However, this capacity, even with dramatic increases of current density, might not be significantly reduced, suggesting that mica-like V_2O_5-nanostructured thin film offers not only fast discharging/charging, but also an excellent rate performance as a promising LIB cathodic electrode. Moreover, even when the current density is 2210 mA g^{-1} (15 C), this V_2O_5 thin-film electrode can still deliver an initial discharge capacity of ~386.6 mAh g^{-1}, much higher than mesoporous V_2O_5 nanofiber's 370 mAh g^{-1} under the lower, 800 mA g^{-1} current density [26]. For all of the present samples, good cyclic stability with a fading rate of less than 1.6%, 1.8%, and 1.5% per cycle was observed, even at the very high current density of 1080 mA g^{-1}, 2210 mA g^{-1}, and 4420 mA g^{-1}, respectively, which results are much better than those reported for nanostructured V_2O_5 in the literature [16,18,27]. In short, the improved discharge capacity, cyclic stability, and rate performance of the mica-like V_2O_5-nanostructured thin film can be attributed to high surface area, short transport distance, its unique structure, and the introduction of oxygen vacancies. The thin films' cyclic stability was further investigated by means of interrupted cyclic testing. Fig. 6b summarizes the cyclic performance of mica-like V_2O_5 nanostructured thin films that underwent five interruptions and repetitive charge/discharge cycles; that is, the same sample was charged/discharged again after the completion of previous continuous charge/discharges. Specifically, a sample was removed from the cell system and let stand in air for one day immediately following an initial test entailing 10 continuous charge/discharge cycles. Then, it was charge/discharged continuously over an additional 10 cycles, following the same procedure according to which the cycle number of the third, fourth, and fifth continuous charge/discharge was also 10, for a total of 50 cycles. It was found that regardless of the repeated interruptions over the course of the 50 charge/discharge test cycles, the discharge capacity of mica-like V_2O_5-nanostructured

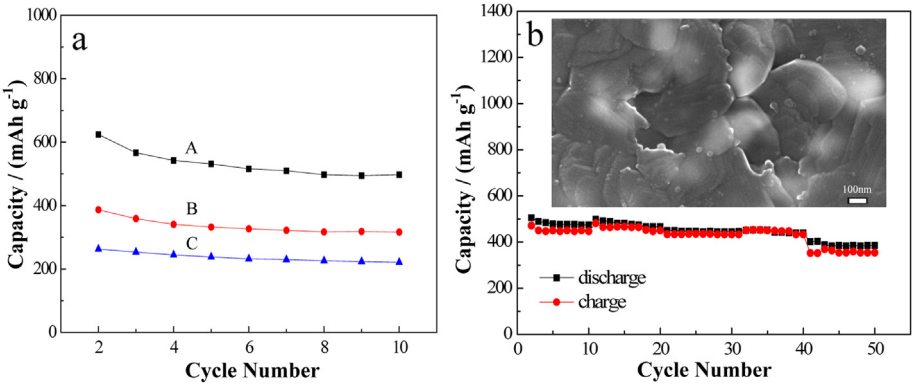

Fig. 6. (a) Relationship between discharge capacity and current density for mica-like V_2O_5-nanostructured thin-film potential ranging from −0.1 to 0.4 V *vs.* Ag/AgCl, A: 1080 mA g^{-1} (7 C), B: 2210 mA g^{-1} (15 C), C: 4420 mA g^{-1} (30 C). (b) Cyclic performance of mica-like V_2O_5-nanostructured thin film for 1080 mA g^{-1} current density and −0.1–0.4 V potential range *vs.* Ag/AgCl.

thin film remained fairly constant: only a very small loss rate was evident, which was less than 0.48% per cycle, lower than that for mesoporous V_2O_5 nanofiber under a lower current density. Indeed, at the 50th and final cycle, the sample could still deliver a discharge capacity of 385.7 mAh g^{-1} under the current density of 1080 mA g^{-1}, which is still higher than the above-noted initial discharge capacity of mesoporous V_2O_5 nanofiber film (370 mAh g^{-1}) under a current density of 800 mA g^{-1} [26]. These results reveal, in summary, that the specific capacity and electrochemical performance of mica-like V_2O_5-nanostructured thin film prepared by the anodic electrodeposition method are superior to those of mesoporous V_2O_5 nanofiber film prepared by electrospinning. Furthermore, the electrodeposition procedure is much simpler and easier to control than that of electrospinning. All in all, anodic-electrodeposited mica-like V_2O_5-nanostructured thin film, due to its excellent electrochemical performance, not to mention its simple, flexible, easily controllable and low-cost processing method, is a promising candidate LIB-cathode material. It should be noted that in the present research, the differences in charge/discharge capacities among the samples were very small, which demonstrated, consistently with the CV test results, the outstanding reversibility of mica-like V_2O_5-nanostructured thin film. Additionally, in the inset of Fig. 6, the SEM image of the thin film after 50 charge/discharge cycles shows that the film morphology did not change, which confirmed films' excellent structural stability. But there occurred erosion on the margin of building blocks, resulting from the dissolution of the nanostructured V_2O_5 in the electrolyte. Thus the mass of active materials on the electrode decreased and the capacities of samples diminished gradually during the charge/discharge cycles.

4. Conclusions

Mica-like V_2O_5-nanostructured thin film was prepared by means of anodic electrodeposition from V_2O_5/H_2O_2 sol solution followed by annealing at 500 °C in air. The film consisted of microstructural mica-like building blocks stacked closely in the form of preferentially oriented orthorhombic V_2O_5 nanosheets of less than 50 nm thickness. With this film, electrolyte infiltration was improved and Li-ion diffusion was facilitated, demonstrating a significantly enhanced Li-ion storage capacity of 596 mAh g^{-1} at the current density of 1080 mA g^{-1}, as well as excellent cyclic stability and reversibility. Such an enhanced lithium-ion intercalation capacity, cyclic stability and rate performance of the V_2O_5 thin-film electrode could be attributed to its unique mica-like morphology, the nanostructure having a higher surface area, shorter Li^+ ion diffusion pathways, and introduced oxygen vacancies.

Acknowledgments

This research work was financially supported in part by the National Natural Science Foundation of China (grant no. 1010200420120076; 11344010). The authors also would like to thank Y.M. Hu and H.S. Gu at Hubei University for the SEM testing and analysis.

Appendix A. Supplementary data

Supplementary data related to this article can be found at http://dx.doi.org/10.1016/j.jpowsour.2014.04.099.

References

[1] E. Pomerantseva, K. Gerasopoulos, X.Y. Chen, G. Rubloff, J. Power Sources 206 (2012) 282.
[2] Y.L. Wang, X.Y. Xu, C.B. Cao, C. Shi, W. Mo, H.S. Zhu, J. Power Sources 242 (2013) 230.
[3] W. Hu, X.C. Du, Y.M. Wu, L.M. Wang, J. Power Sources 237 (2013) 112.
[4] Y.N. Ko, J.H. Kim, S.H. Choi, Y.C. Kang, J. Power Sources 211 (2012) 84.
[5] G. Wei, T.E. Haas, R.B. Goldner, Solid State Ionics 58 (1992) 115.
[6] M.E. Donders, W.M. Arnoldbik, H.C.M. Knoops, W.M.M. Kwssels, P.H.L. Notten, J. Electrochem. Soc. 160 (2013) A3066.
[7] B. Xu, D.N. Qian, Z.Y. Wang, Y.S. Meng, Mater. Sci. Eng. R 73 (2012) 51.
[8] H.T. Huang, P.G. Bruce, J. Power Sources 54 (1995) 52.
[9] S.F. Yang, P.Y. Zavalij, M.S. Whittingham, Electrochem. Commun. 9 (2001) 505.
[10] R. Malik, A. Abdellahi, G. Ceder, J. Electrochem. Soc. 160 (2013) A3179.
[11] S.M. Dou, W.L. Wang, J. Solid State Electrochem. 15 (2011) 399.
[12] X.L. Meng, S.M. Dou, W.L. Wang, J. Power Sources 184 (2008) 489.
[13] C.H. Chen, J. Liu, M.E. Stoll, G. Henriksen, D.R. Vissers, K. Amine, J. Power Sources 128 (2004) 278.
[14] Y.K. Sun, Z.H. Chen, H.J. Noh, D.J. Lee, H.G. Jung, Y. Ren, S. Wang, C.S. Yoon, S.T. Myung, K. Amine, Nature 11 (2012) 942.
[15] S.R. Li, S.Y. Ge, Y. Qiao, Y.M. Chen, X.Y. Feng, J.F. Zhu, C.H. Chen, Electrochim. Acta 64 (2012) 81.
[16] Y. Wang, G.Z. Cao, Adv. Mater. 20 (2008) 2251.
[17] K. Lee, Y. Wang, G.Z. Cao, J. Phys. Chem. B 109 (2005) 16700.
[18] Y.Y. Liu, M. Clark, Q.F. Zhang, D.M. Yu, D.W. Liu, J. Liu, G.Z. Cao, Adv. Energy Mater. 1 (2011) 194.
[19] C.J. Fontenot, J.W. Wiench, G.L. Schrader, J. Phys. Chem. B 104 (2000) 11622.
[20] Y. Wang, H.M. Shang, T. Chou, G.Z. Cao, J. Phys. Chem. B 109 (2005) 11361.
[21] V. Petkov, P.N. Trikalitis, E.S. Bozin, S.J.L. Billinge, T. Vogt, M.G. Kanatzidis, J. Am. Chem. Soc. 124 (2002) 10157.
[22] J. Livage, Chem. Mater. 3 (1991) 578.
[23] J.J. Legendre, P. Aldebert, N. Baffier, J. Livage, J. Colloid Interface Sci. 94 (1983) 84.
[24] P.P. Prosini, S. Passerini, R. Vellone, W.H. Smyrl, J. Power Sources 75 (1998) 73.
[25] K.T. Lee, J. Cho, Nanotoday 6 (2011) 28.
[26] D.M. Yu, C.G. Chen, S.H. Xie, Y.Y. Liu, K. Park, X.Y. Zhou, Q.F. Zhang, J.Y. Li, G.Z. Cao, Energy Environ. Sci. 4 (2011) 858.
[27] K. Takahashi, Y. Wang, G.Z. Cao, J. Phys. Chem. B 109 (2005) 48.
[28] G. Strukul, Catalytic Oxidations with Hydrogen Peroxide as Oxidant, Kluwer Academic Pulishers, Dordrecht, The Netherlands, 1991.
[29] Y.H. Zhang, P. Xiao, X.Y. Zhou, D.W. Liu, B.B. Garcia, G.Z. Cao, J. Mater. Chem. 19 (2009) 948.
[30] D.M. Yu, S.T. Zhang, D.W. Liu, X.Y. Zhou, S.H. Xie, Q.F. Zhang, Y.Y. Liu, G.Z. Cao, J. Mater. Chem. 20 (2010) 10841.